

Active Agents in Heterogeneous Photocatalysis: Atomic Oxygen Species vs. OH· Radicals: Related Quantum Yields

by Jean-Marie Herrmann

Laboratoire de Photocatalyse, Catalyse et Environnement, IFOS (UMR CNRS n° 5621);
Ecole Centrale de Lyon, BP 163, F-69131 Ecully Cédex
(phone: (33) 472 186493; fax: (33) 478 330337; e-mail: jean-marie.herrmann@ec-lyon.fr)

Dedicated to Professor *André M. Braun* on the occasion of his 60th birthday

After a general survey of the fundamental characteristics of heterogeneous photocatalysis, the present article classifies the ensemble of reactions into three major categories: *i*) mild oxidations, *ii*) total oxidations, and *iii*) reactions involving hydrogen. Depending on the presence or absence of H₂O, the active oxidizing species will be either a dissociated neutral oxygen species, denoted as O*, which is present in anhydrous systems and responsible for selective mild oxidation reactions, or an OH· radical, formed in the presence of H₂O and responsible for totally degradative oxidation reactions. The existence of O* species is substantiated by photoconductivity measurements, oxygen-isotope exchange, and reactions in which oxygen-free NO is the oxidizing agent. The influence of the five main parameters that govern kinetics experiments *i*) the mass of the catalysts, *ii*) the wavelength, *iii*) the concentrations or partial pressures of reactants, *iv*) the temperature, and *v*) the radiant flux is examined to determine the best conditions for obtaining the optimum photocatalytic quantum yield (POY), the definition of which is based on the quantum yield given in [1] for photochemistry.

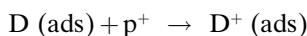
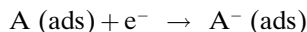
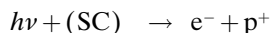
1. Introduction. – Heterogeneous photocatalysis is a discipline that includes a large variety of reactions: selective mild oxidations, total oxidations, dehydrogenation, hydrogen transfer, ¹⁶O₂ – ¹⁸O₂ and alkane-deuterium isotopic exchange, noble metal deposition for separation and recovery, water detoxification, gaseous pollutant removal, *etc.* In line with the two latter points, photocatalysis can be considered one of the new ‘Advanced Oxidation Technologies’ (AOT) for air and water purification treatment. Several books and reviews have been recently devoted to this problem [2–7]. A recent review reported more than 1700 references on the subject [8] and constitutes the basic reference for the best exhaustive report of global activity on heterogeneous photocatalysis.

Heterogeneous photocatalysis can be carried out in various media: gas phase, pure organic liquid phase, or aqueous solution. As for classical heterogeneous catalysis, the overall process can be broken down into five independent steps: *1*) transfer of the reactants from the fluid phase to the surface, *2*) adsorption of at least one of the reactants, *3*) reaction in the adsorbed phase, *4*) desorption of the product(s), or *5*) removal of the products in the fluid phase.

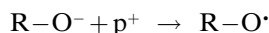
The photocatalytic reaction occurs in the adsorbed phase during *Step 3*). The only difference with conventional catalysis is the mode of activation of the catalyst, in which the thermal activation is replaced by a photonic activation as developed in the next section. The activation mode is not concerned with the remaining steps, although photo-adsorption and photo-desorption of some reactants, mainly oxygen [9] and oxygen-free NO [10], does occur.

2. Fundamentals of Heterogeneous Photocatalysis. – 2.1. *Principle of Heterogeneous Photocatalysis.* When a semiconductor catalyst (SC) of the chalcogenide type (oxides (TiO_2 , ZnO , ZrO_2 , CeO_2 , ...), or sulfides (CdS , ZnS , ...)) is illuminated with photons whose energy is equal to or greater than their band-gap energy E_G ($h\nu \geq E_G$), the absorption of these photons by the solid occurs and is followed by the creation, within the bulk, of electron-hole pairs, which dissociate into free photoelectrons in the conduction band and photoholes in the valence band, the photoholes being virtual positive-charge carriers corresponding to an electron vacancy in the pool of lattice anions (O^{2-} in oxides and S^{2-} in sulfides).

Simultaneously, in the presence of a fluid phase (gas or liquid), a spontaneous adsorption occurs and, according to the redox potential (or energy level) of each adsorbate, electron transfer proceeds towards acceptor molecules, whereas positive photoholes are transferred to donor molecules (actually the hole transfer corresponds to the cession of an electron by the donor to the solid).



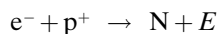
Each ion formed subsequently reacts to form the intermediates and final products. Gaseous acceptor species can be O-species and/or O_2 molecules [9] and O_2 -free NO [10]. In H_2O , H_2O_2 and/or $\text{S}_2\text{O}_8^{2-}$ can be considered electrophilic reactants or electrons scavengers [11]. Donor species can be either negatively charged ionsorbates such as O^- , O_2^- , NO^- , and OH^- , or organic molecules such as alcohols and carboxylic acids, both dissociated in their reactive adsorbed states:



the last reaction being known as the ‘photo-Kolbe’ reaction.

As a consequence of the three reactions above, the photonic excitation of the catalyst appears to be the initial step of the activation of the whole catalytic system. Thence, the efficient photon has to be considered a reactant and the photon flux a special fluid phase, the so called ‘electromagnetic phase’ [12]. The photon energy is adapted to the absorption of the catalyst, not to that of the reactants. The activation of the process proceeds *via* excitation of the solid rather than that of the reactants: *there is no photochemical process in the absorbed phase but only a true heterogeneous photocatalytic regime, as demonstrated further.*

The photoefficiency can be reduced by electron-hole recombination, which corresponds to loss of the photoelectronic energy as heat.

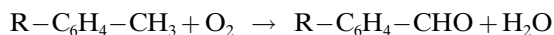


(N: neutral center; E: dissipated energy (light $h\nu' \leq h\nu$ or heat))

2.2. *Photocatalysts.* Various chalcogenides (oxides and sulfides) have been used: TiO_2 , ZnO , CeO_2 , CdS , ZnS , etc. As generally observed, the best photocatalytic performance with maximum quantum yields are always obtained with TiO_2 , since it better combines its adsorptive properties with respect to reactants with its absorptive properties with respect to photons [6]. In addition, anatase is the most active allotropic form of TiO_2 among the various ones available, either natural (rutile and brookite) or artificial ($\text{TiO}_2\text{-B}$, $\text{TiO}_2\text{-H}$). Anatase is thermodynamically less stable than rutile, but its formation is kinetically favored at lower temperature ($< 600^\circ$). This lower synthesis temperature could account for a higher surface area and a higher surface density of active sites for adsorption and for catalysis. It is generally admitted that the surface sites of titania, especially in aqueous medium, can be considered as surface OH groups, identified and titrated by the pioneer work of Böhm [13]. In most of the systems described in the literature, the catalyst used was mainly anatase and, in particular, titania (*Degussa TiO₂ P-25*, 50 m²/g, 70–80% anatase). The systems described below will concern this photocatalyst, unless otherwise stated.

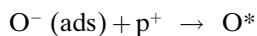
3. Main Types of Photocatalytic Reactions. – 3.1. *Mild Oxidation Reactions.* The gas-phase oxidations in which O_2 in air is the oxidizing agent mainly concern the mild oxidation of alkanes, alkenes, and alcohols to aldehydes and ketones [14]. Inorganic gases such as CO , NH_3 or H_2S could also be oxidized: NH_3 was oxidized mainly to N_2 [15]. NO could be photocatalytically decomposed into N_2 at low pressures and into N_2O at higher pressures, whereas the O_2 generated could be used to oxidize butanols to butanal and butanone [10].

Liquid-phase reactions concerned the selective mild oxidation of liquid hydrocarbons (alkanes, alkenes, cycloalkanes, aromatics) to aldehydes and ketones [16a]. For instance, cyclohexane and decahydronaphthalene were oxidized to cyclohexanone and octahydronaphthalen-2-one, respectively, with identical selectivities of 86% [16b]. Aromatic hydrocarbons [17] such as alkyltoluenes or *o*-xylenes were selectively oxidized on the Me group into alkylbenzaldehydes:



Pure liquid alcohols were also oxidized to their corresponding aldehydes or ketones. In particular, the oxidation of *i*-PrOH to acetone was chosen as a photocatalytic test for measuring the efficiency of passivation of TiO_2 - or ZnO -based pigments in painting against weathering.

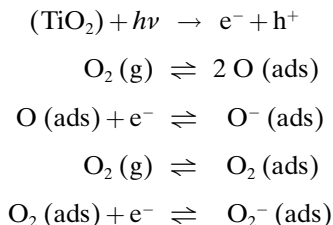
The high selectivity was ascribed to a photoactive neutral, atomic oxygen species [14–18]



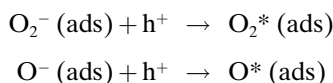
The existence of such a dissociated activated species was put into evidence by various means, mainly based on photoconductivity measurements.

The creation of photo-electrons and holes can be directly detected by photoconductivity σ measurements. The variation in σ as a function of the incident photon's wavelength was found to be parallel to the absorbance of the catalyst. Under O_2 , σ was

found to vary as a function of $P_{\text{O}_2}^{-1/2}$ at low (decreasing) pressures and as $P_{\text{O}_2}^{-1}$ at higher P_{O_2} . This has been ascribed to dissociative and associative O_2 ionosorption



In a pure organic (gaseous or liquid) phase, O_2 ionosorbates are the only negatively charged species able to react with holes.



The reaction heat is partially dissipated by O_2 desorption, which is endothermic. However, what is the active one in partial mild oxidation?

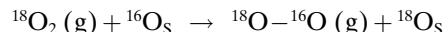
In situ photoconductivity σ measurements were performed in a photoreactor-cell, specially designed to simultaneously follow σ and the reaction rates as a function of the partial pressures of reactants, in the partial oxidation of isobutane to acetone.

The results were:

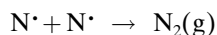
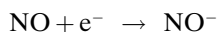
$$\begin{aligned}\sigma &= k P_{\text{O}_2}^{-1} P_1^0 \\ r &= k' P_{\text{O}_2}^0 P_1^{0.35}\end{aligned}$$

The partial orders of both reactants with respect to σ clearly indicated that the alkane has no electronic interactions with titania ($\sigma \propto P_1^0$), whereas O_2 is mainly adsorbed as the O_2^- species. By contrast, isobutane has a partial order (0.35) with respect to the reaction rate. This is in line with a *Langmuir-Hinshelwood* mechanism with $r = k \theta_1 = k K P_1 / (1 + K P_1) \approx k K' P_1^{0.35}$.

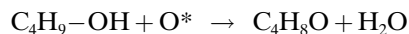
Oxygen is zero order with respect to r , whereas its order with respect to σ is -1 , indicative of the presence of $\text{O}_2^-(\text{ads})$ species. The conclusion was reached that, although O_2^- species are present, they are not the active species in mild oxidation reactions; these are instead assumed to be dissociated activated O^* species, as has been corroborated by various observations: 1) Oxygen isotopic exchange (OIE) followed the 'R' mechanism' based on the existence of a dissociated oxygen species ($^{16}\text{O}_s$) at the surface:



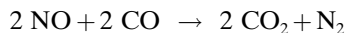
2) The same OIE performed in the presence of isobutane initiated only when isobutane had totally reacted, clearly indicating the concurrence for the same species. 3) Mild oxidation reactions could be performed with O_2 -free NO acting as a source of O-atoms according to:



O^* could be used *in situ* as the oxidizing agent *i*) of BuOH to butanone [10]



and *ii*) also of CO to CO_2 [19] as illustrated in *Fig. 1*.



Besides the experimental contribution to proof the existence of dissociated oxygen species, this reaction indicates that two toxic gases could be eliminated by conversion to two innocuous ones, CO_2 and N_2 , in an anaerobic gas phase. 4) All the photoactive oxide catalysts, besides titania, *viz.* ZrO_2 , ZnO , CeO_2 , Sb_2O_4 , exhibited dependence of σ on $\text{P}_{\text{O}_2}^{-1/2}$ [9].

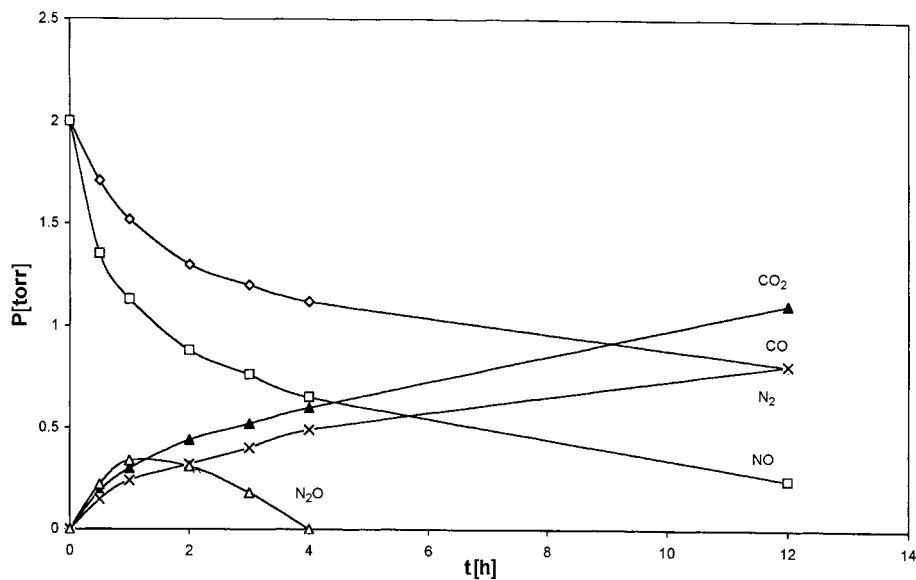
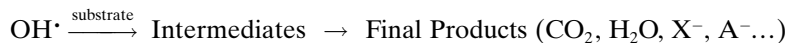
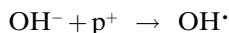


Fig. 1. Photocatalytic oxidation of CO to CO_2 by NO in contact with UV-irradiated titania (Degussa P-25). Partial pressures 1 Torr; CO (◇), NO (□), CO_2 (▲), N_2 (×), N_2O (△).

3.2. *Total Oxidation Reaction in Aqueous Phase.* The selective mild oxidation reaction could be obtained in pure gaseous or liquid organic phases. By contrast, as soon as H_2O is present, the selectivity changes to favor total oxidative degradation. This was ascribed to the photogeneration of stronger, unselective, oxidant species, namely OH^{\cdot} radicals originating from H_2O via the OH^- groups on titania's surface. In aqueous media, because of the high concentration of H_2O (55.55 mol/l) and of the highly hydrophilic character of titania, its surface can be assumed to be saturated not only in chemisorbed H_2O but especially in OH^- groups, whose coverage at saturation is

estimated to be equal to $5 \times 10^{18}/\text{m}^2$ [13]. These OH^- groups are continually renewed by the ionic dissociation of H_2O , and constitute the main negatively charged species that react with holes:

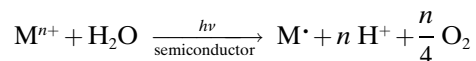


This system is the most promising issue for application of heterogeneous photocatalysis, since it is directly connected to water detoxification and to pollutant removal in aqueous effluents.

The most spectacular results were obtained in the field of organic-pollutants removal [2–8]. OH^\bullet Radicals are especially efficient in the destruction of aromatic contaminants since they are able to substitute heteroatoms such as halides on an aromatic ring to give the corresponding phenolic compounds. An example is given for the degradation of pesticide tetrachlorvinphos in *Scheme 1*.

Similarly, various toxic anions can be oxidized into harmless or less toxic compounds with TiO_2 as the photocatalyst. For instance, nitrite is oxidized to nitrate [20][21], phosphite to phosphate [22], and sulfide to sulfite [23], and thiosulfate [24] to sulfate, whereas cyanide is converted either to isocyanide [25], N_2 [26], or nitrate [27].

Heavy metals are generally toxic and can be removed from industrial waste effluents [24][28–31] as small crystallites deposited on the photocatalyst according to:

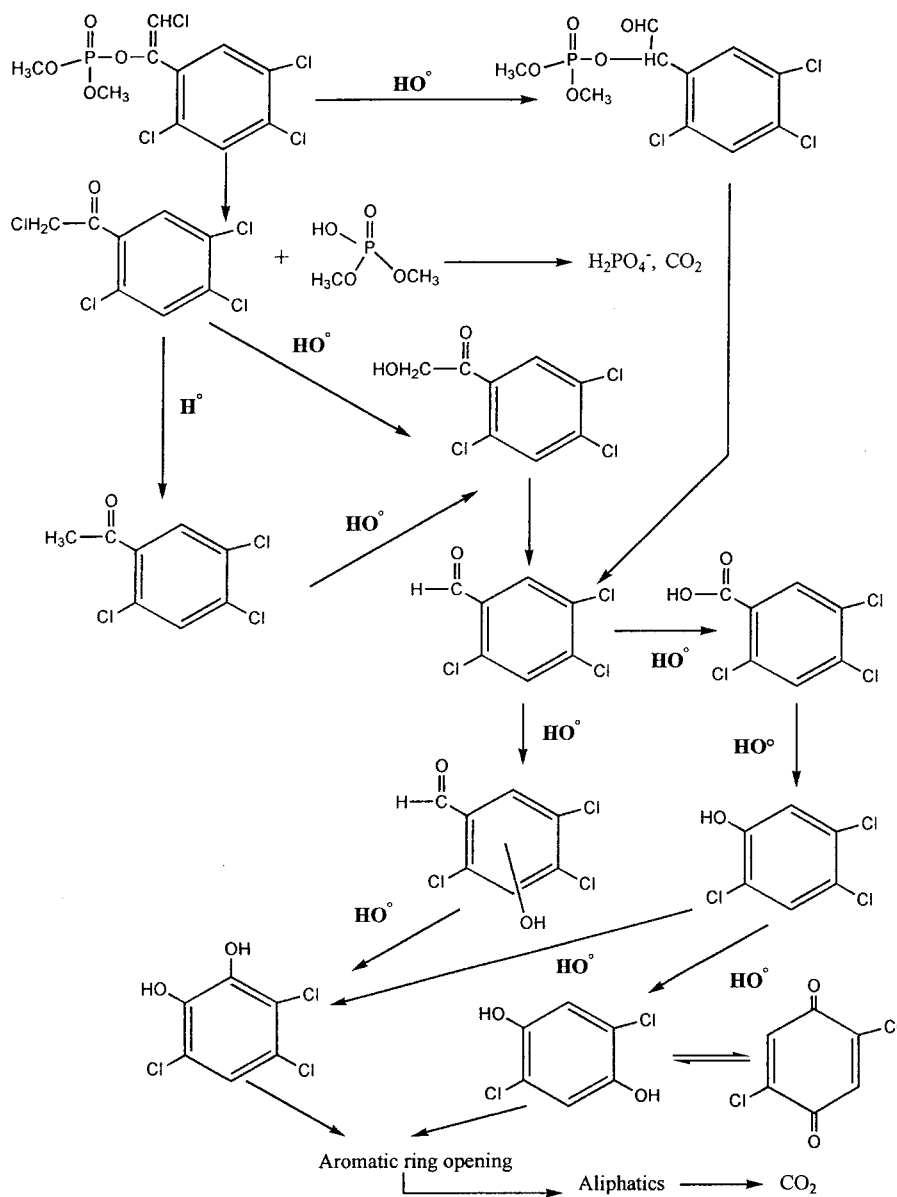


provided the redox potential of the cation metal couple is higher than the flat-band potential of the semiconductor. Under identical conditions, the following reactivity pattern was found: $\text{Ag} > \text{Pd} > \text{Au} > \text{Pt} \gg \text{Rh} \gg \text{Ir} \gg \text{Cu} = \text{Ni} = \text{Fe} = 0$. Whereas photoelectrons were consumed to reduce the noble metals, photoholes oxidized H_2O to O_2 via the neutralization of OH^- by holes.

2.3. Photocatalytic Reactions Involving Hydrogen. In photocatalytic reactions involving hydrogen, either as a reactant (deuterium-alkane isotopic exchange (DAIE) [32]) or as a product (alcohol dehydrogenation [33]), the system requires the presence of a metal to act as a cocatalyst to *i*) dissociate the reactant (D_2) and *ii*) recombine H and D into H_2 , HD, or D_2 . Additionally, the metal *i*) attracts electrons by photoinduced metal-support interaction (PMSI), *ii*) decreases the electron-hole recombination, and *iii*) makes the reaction run catalytically as exemplified by the two cyclic mechanisms in *Schemes 2* and *3*. In *Scheme 2*, it appears clearly that DAIE occurs via deuterated hydroxyl radicals (OD^\bullet), whereas in *Scheme 3*, alcohols react directly with holes because of their dissociative adsorption as alcoholate plus a proton.

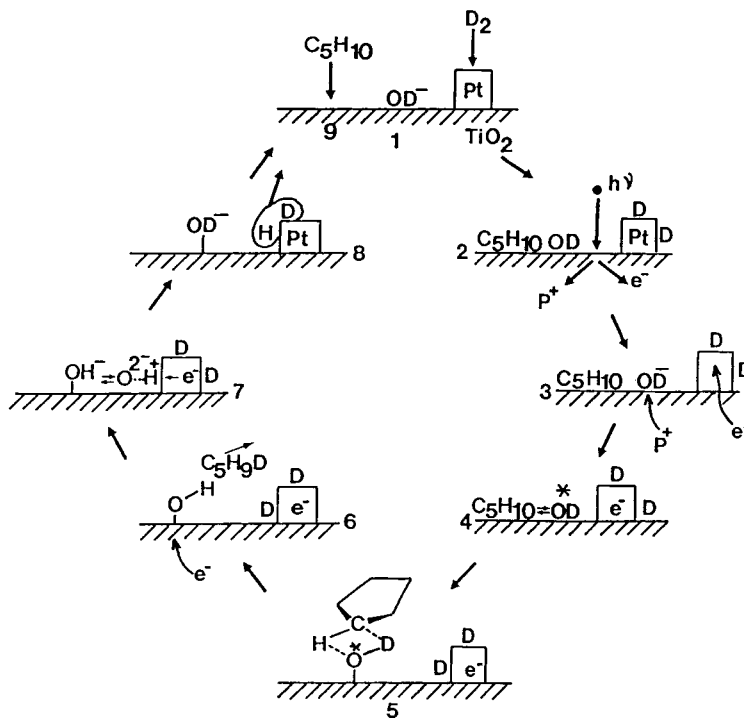
4. O^* vs. OH^\bullet Reactivities. – From the above considerations, two oxidizing active species can be generated at the surface of UV-irradiated titania, depending on the reaction medium.

In anhydrous media, mild oxidation reactions can be obtained that lead to very high selectivities. By contrast, in the presence of H_2O (or of humid air), selectivities change

Scheme 1. *Tetrachlorvinphos Degradation before the Opening of the Aromatic Ring*

from partial to total oxidation and, generally, final products can reach their upper – often harmless – oxidation states. This is true for both organic and inorganic compounds.

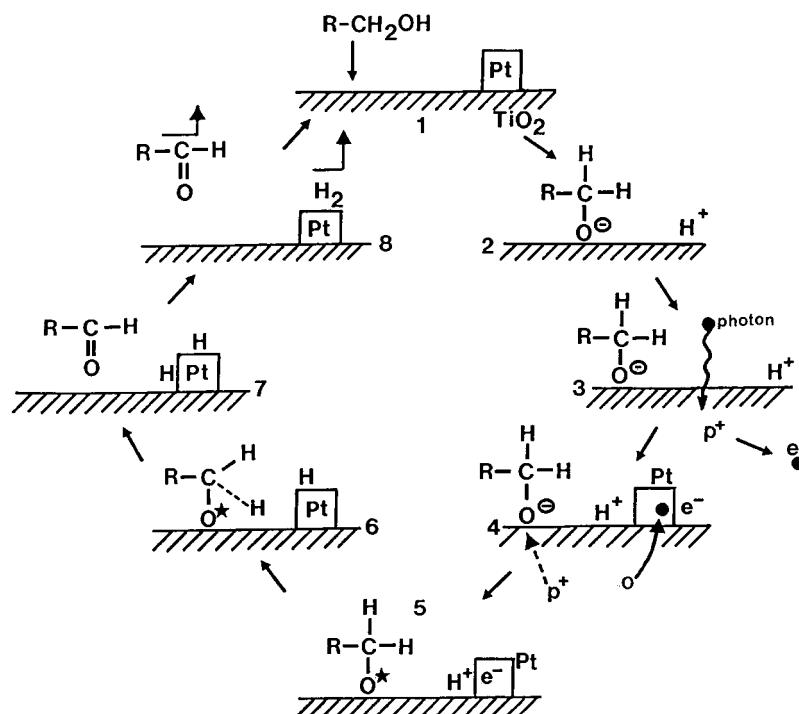
For instance, dry gaseous NH_3 was found to oxidize mainly to N_2 (selectivity of 80%) [14], whereas NH_4^+ is oxidized to nitrate *via* nitrite ions in aqueous solution. Similarly, dry *o*-xylene is 100% oxidized to 2-methylbenzaldehyde, whereas, with

Scheme 2. *Eight-Step Cyclic Mechanism of Deuterium-Cyclopentane Isotopic Exchange on UV-Irradiated Pt/TiO₂ Catalyst*

humid air, it is oxidized to CO₂ via the formation of phenolic intermediates [34]. This reaction has been selected as a model reaction to illustrate the fate of aromatic hydrocarbons in the (humid) atmosphere in the presence of solid aerosols originating from fly ash [34].

5. Examination of Common Physical Parameters Governing the Kinetics of Photocatalytic Reactions. – Whichever reaction is considered among the very different ones described above, all follow common physicochemical laws, whose expressions are summarized in the five diagrams of Fig. 2.

5.1. *Mass of the Catalyst.* Either in static, or in slurry, or in dynamic-flow photoreactors, the initial rates of reaction (r) were found to be directly proportional to the mass (m) of catalyst (Fig. 2, a). This is indicative of a true heterogeneous catalytic regime in which r increases proportionally with the total surface area exposed ($S_T = S_{\text{BET}} \times m$), i.e., with the total number of surface sites. However, above a certain value of m , r levels off and becomes independent of m . This limit depends on the geometry and on the working conditions of the photoreactor (catalytic bed, volume, light flux, ...), and was found to be equal to 2.5 mg TiO₂ per cm³ of suspension (2.5 g/l) in the static photoreactor described in Fig. 3. This optimum value was found to be equal to 1.3 mg TiO₂/cm² deposited on a plate of the fixed bed [35] and to 0.2 g/l in the solar photoreactor at *Plataforma Solar de Almeria* (Spain) [11][36]. These limits correspond

Scheme 3. Eight-Step Cyclic Mechanism of Alcohol Dehydrogenation on UV-Irradiated Pt/TiO₂ Catalyst

to the maximum amount of TiO₂ that can be totally illuminated. For higher quantities of catalyst, a screening effect of excess particles occurs, which masks part of the photosensitive surface. In some cases, a high excess of mass of titania has even been found to decrease the reaction rate beyond the plateau of Fig. 2, a. This has been thought to be related to increased scattering of photons out of the reactor as catalyst concentration near the reaction wall is increased, as has already been reported [37].

For any study or application, this optimum mass of catalyst has to be chosen *i*) to avoid an useless excess of catalyst and *ii*) to ensure total absorption of efficient photons. This value can vary over a rather wide range, *e.g.*, from 2.5 g TiO₂/l in laboratory experiments, with a batch photoreactor, down to 0.2 g/l for the CPC solar reactor at PSA [11][36], which is a recirculation plug flow reactor corresponding to a batch reactor. Actually, this optimum varies with the optical pathway within the suspension.

5.2. Wavelength. The variation in r as a function of the wavelength (λ) follows the absorption spectrum of the catalyst (Fig. 2, b), with a threshold corresponding to its band-gap energy. For TiO₂ having $E_G = 3.02$ eV, this requires $\lambda \leq 400$ nm, *i.e.*, near-UV wavelength (UV-A). In addition, it must be ensured that the reactants do not absorb light so that exclusively the catalyst undergoes photoactivation for a true heterogeneous catalytic regime (no homogeneous catalysis nor any photochemistry in the absorbed phase). Actually, the variations $r = f(\lambda)$ can only be obtained with sensitive reactions such as ¹⁶O₂–¹⁸O₂ isotopic exchange [10] or facile reactions having a high quantum yield (defined further), such as MeOH dehydrogenation [33].

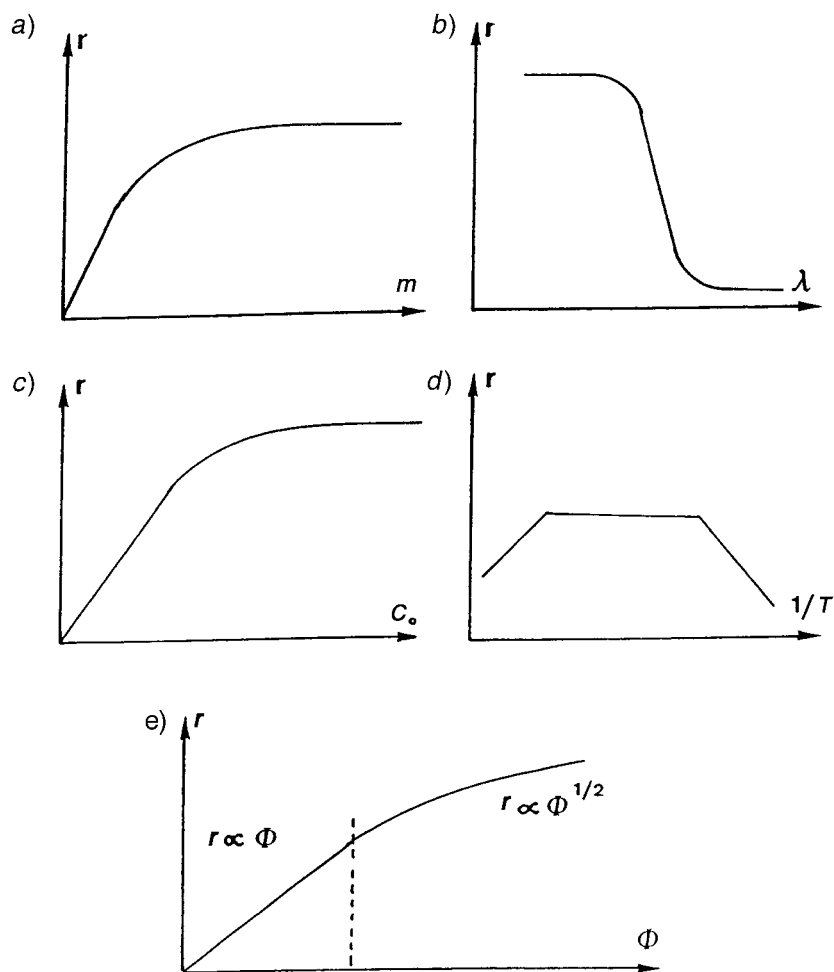


Fig. 2. Variation in photocatalytic activity of a solid, as estimated by the reaction rate (r) as a function of the five basic parameters that govern the kinetics. a) Mass of catalyst, b) wavelength, c) concentration (or partial pressure), d) temperature (expressed as its reciprocal in an Arrhenius plot), and e) radiant flux (in W/m^2).

5.3. *Concentrations and/or Partial Pressures.* Generally, the kinetics formally follows a *Langmuir-Hinshelwood* mechanism, confirming the heterogeneous-catalytic character of the system with the rate r varying proportionally with the coverage θ as:

$$r = k \theta = k (K C / (1 + K C))$$

where k is the true rate constant and K is the adsorption constant. Two limiting cases are often encountered. For dilute solution, when the product KC becomes $\ll 1$, the reaction becomes apparently first order.

$$r \approx k K C = k_{\text{app}} C$$

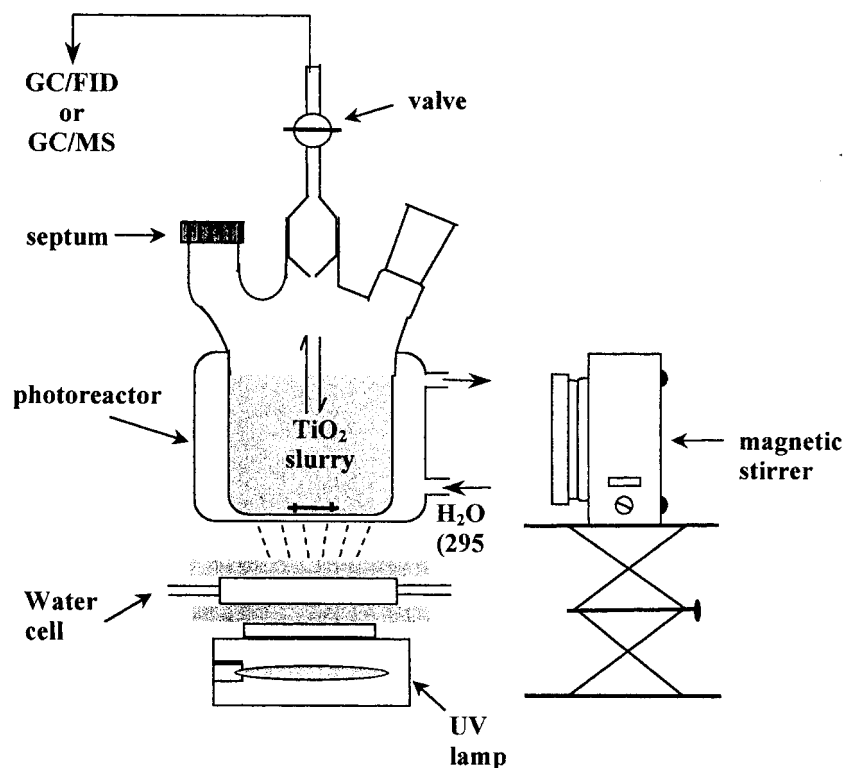


Fig. 3. Schematic diagram of a laboratory-scale batch slurry photoreactor used for mild oxidation of organics, oxidative water decontamination, and alcohol dehydrogenation

On the contrary, for high concentrations when KC becomes $\gg 1$, the surface coverage becomes saturated. Correspondingly, the reaction appears to be zero order and r is maximum and equal to k (Fig. 2,c). In between, the reaction order with respect to concentration varies between 1 and 0. Over a narrow enough concentration range, the homographic function $\theta = k (KC/(1 + KC))$ can be assimilated to a power function $\theta = k C^a$, where a is constant and $0 < a < 1$.

For gas-phase reactions, similar *Langmuir-Hinshelwood* expressions are found, which are expressed with partial pressures P instead of C . Kinetic studies can provide information about the mode of adsorption of the reactant. In some cases, such as in liquid alcohol dehydrogenation [33], r follows variations including the square root of the concentration:

$$r = k [K^{1/2} C^{1/2} / (1 + K^{1/2} C^{1/2})]$$

This indicates that the reactant is in a dissociated adsorbed state. For maximum yield, reactions should be performed with initial concentrations equal to or higher than the threshold of the plateau ($C_0 \geq ca. 5 \times 10^{-3} M$). In reactions to purify and detoxify water, pollutant concentrations are generally (and fortunately) low, and r is expected to be substantially lower than the optimum value at surface saturation.

5.4. *Temperature.* Because of the photonic activation, the photocatalytic systems do not require heating and are operating at room temperature. The true activation energy E_t is zero, whereas the apparent activation energy E_a is often very small (a few kJ/mol) in the medium temperature range ($20^\circ \leq \theta \leq 80^\circ$). However, at very low temperatures ($-40^\circ \leq \theta \leq 0^\circ$), the activity decreases and the apparent activation energy E_a becomes positive (Fig. 2, d). By contrast, at ‘high’ temperatures ($\theta \geq 70-80^\circ$) for various types of photocatalytic reactions, the activity decreases and the apparent activation energy becomes negative (Fig. 2, d). This behavior can be easily explained within the framework of the *Langmuir-Hinshelwood* mechanism described above for $r=f(C)$. The decrease in temperature favors adsorption, which is a spontaneous exothermic phenomenon. In the rate equation, θ tends to unity, whereas KC becomes $\gg 1$. In addition, lowering T also favors adsorption of the final reaction product P, whose desorption tends to become the rate-limiting step. Therefore, r becomes:

$$r = k \theta = k K C / (1 + K C + K_p C_p) \approx k / K_p C_p$$

where K_p is the adsorption constant of final product P. Correspondingly, the apparent activation energy E_a becomes equal to:

$$E_a = E_t - \Delta H_p$$

i.e., to the sum of the true activation energy E_t (theoretically equal to zero because of the photonic-activation mode of the catalysts) and of the enthalpy of adsorption of product P, which is negative ($\Delta H_p = -Q_p$, Q_p being the heat of adsorption counted positive):

$$E_a = E_t + Q_p \approx 0 + Q_p = Q_p$$

This relationship was demonstrated for reactions involving H_2 (alcohol dehydrogenation [33] or deuterium-alkane isotopic exchange [32]), which are carried out on bifunctional Pt/TiO₂ photocatalysts. E_a was found equal to +10 kcal/mol (+42 kJ/mol), which is just equal to the heat $Q_{H_2(ads)}$ (or to the opposite of the enthalpy $\Delta H_{H_2(ads)}$) of the reversible adsorption of H_2 on Pt measured by microcalorimetry [38]:

$$E_a = E_t - \Delta H_{H_2(ads)} = 0 + Q_{H_2(ads)} = +10 \text{ kcal/mol}$$

On the contrary, when θ increases above 80° and approaches the boiling point of H_2O , the exothermic adsorption of reactant A becomes disfavored and tends to become the rate-limiting step, with r becoming:

$$r = k \theta = k K C / (1 + K C) \sim k K C$$

Correspondingly, the apparent activation energy becomes:

$$E_a = E_t + \Delta H_A = 0 - Q_A < 0$$

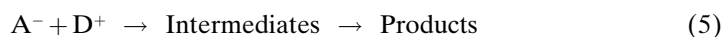
This indicates that the adsorption of the reactant A becomes the rate-limiting step.

$$E_a = E_t - \alpha Q_A = 0 - \alpha Q_A < 0,$$

with α being a coefficient that varies progressively from 0 to 1 as the temperature increases and as adsorption of reactant A becomes more and more the rate-limiting step.

As a consequence, the optimum temperature is generally 20–80°, *explaining why previous solar devices that use sunlight concentrators including IR beams require coolers* [39]. That it is unnecessary to heat the catalyst to activate it is attractive for photocatalytic reactions carried out in aqueous media and, in particular, for environmental purposes (photocatalytic water purification). There is no need to waste energy in heating water, which possesses a high heat capacity, and explains why photocatalysis is cheaper than incineration [40].

5.5. *Radiant Flux.* In laboratory experiments, the artificial light power used was determined by measuring the efficient radiant flux Φ (in mW/cm²) with a radiometer, and corresponded to 21% of the electrical power consumed. It has been shown for all types of photocatalytic reactions that r is proportional to the radiant flux Φ (Fig. 2, e). This confirms the photoinduced nature of the activation of the catalytic process, with the participation of photoinduced electrical charges (electrons and holes) in the reaction mechanism. However, above a certain value, which varies for each photo-system used, r becomes proportional to $\Phi^{1/2}$. This can be demonstrated with the following five basic equations:



and the rate-limiting step is the reaction in the adsorbed phase (*Eqn. 5*) according to a *Langmuir-Hinshelwood* mechanism. Therefore

$$r = r_5 = k_5 [\text{A}^-] [\text{D}^+] \quad (6)$$

In an n-type semiconductor such as titania, the photoinduced-hole concentration is much smaller than that of electrons, including both photoinduced electrons and n-type electrons originating from titania's oxygen substoichiometry: $[p^+] \ll [e^-]$. Therefore holes are the limiting active species. Thence:

$$r = r_5 = r_4 = k_4 [\text{D}] [p^+] \quad (7)$$

At any instant, one has:

$$d[p^+]/dt = r_1 - r_2 - r_4 = 0 = k_1 \Phi - k_2 [e^-] [p^+] - k_4 [\text{D}] [p^+] \quad (8)$$

Thence:

$$[p^+] = \frac{k_1 \Phi}{k_2 [e^-] + k_4 [D]} \quad (9)$$

and

$$r = \frac{k_1 k_4 [D] \Phi}{k_2 [e^-] + k_4 [D]} = \frac{k_1 k_4 [D] \Phi}{K_4 [D] + k [e^-]} \quad (10)$$

From the *Eqn. 10*, it can be seen that r is directly proportional to the Φ .

In the case of high fluxes, the instantaneous concentrations $[e^-]$ and $[p^+]$ become much larger than $k_4 [D]$. Therefore *Eqn. 9* becomes:

$$[p^+] \sim \frac{k_1 \Phi}{k_2 [e^-]} \quad \text{with } [p^+] \sim [e^-] \quad (11)$$

Thence:

$$[p^+]^2 \sim k_1 \Phi / k_2 \quad (12)$$

From *Eqns. 7 and 12*, r becomes:

$$r = r_5 = r_4 = k_4 [D] (k_1 \Phi / k_2)^{1/2} \quad (13)$$

which means that r is proportional to $\Phi^{1/2}$ and that the rate of electron-hole formation becomes greater than the photocatalytic rate. Since the electron-hole recombination is a bimolecular reaction process, the second-order rate is favored by an increase in concentrations. This means that r becomes dominated by the electron-hole recombination. Although r is still increasing with radiant flux, most of photons generate electrical charges that recombine, thus dissipating noble UV-light energy into useless heat. The optimal light-power utilization corresponds to the domain where r is proportional to Φ , and it is of a paramount importance to determine it in any photocatalytic device aimed at optimal use of photons.

In laboratory experiments, near-UV light was provided by a *Philips* UV-lamp (*HPK 125* watts), described in [1] and placed in front of the optical window of the photoreactor as described in *Fig. 3*. IR Beams were removed with a circulating-water cell. The wavelength domain was adjusted with optical filters (fused silica, or *Pyrex*, or *Corning* glass filters), and the radiant flux was measured with a radiometer (*Radiometer Technology Model 21A*) calibrated against a calorimeter. Under these conditions, a transition value of 25 mW/cm² was found for Φ , *e.g.*, in the oxidation of cyclohexane in cyclohexanone [16a]. It should be noted that the rate is proportional to the efficient photon flux, *i.e.*, to the total number of incident photons able to create electron-hole pairs. However, for a given light source, the efficient part of the spectrum remains constant. This is why r is apparently proportional to the overall incident radiant flux Φ_T .

5.6. Influence of O₂ Pressure in Oxidation Reactions. The influence of O₂ pressure is easily determined in gas-phase reactions. For instance, in the mild photocatalytic oxidation of alkanes to aldehydes and/or ketones, it was found that the reaction was zero-order in O₂, indicating a total surface coverage of this gas [18]. Photoconductivity

measurements indicated that O_2 was photoadsorbed as O_2^- [18]. For liquid-phase reactions, it was difficult to study the influence of P_{O_2} because the reaction is polyphasic. It is generally assumed that O_2 is adsorbed on titania from the liquid phase, where it is dissolved according to *Henry's law*. If O_2 is continually supplied to the aqueous suspension, it can be assumed that its coverage at the surface of titania is constant and can therefore be integrated into the apparent rate constant:

$$A + O_2 \rightarrow P$$

$$r_A = -d[A]/dt = k \theta_A \theta_{O_2} = k_{app} \theta_A$$

Actually, the apparent rate constant is a function of the power flux and of the O_2 coverage. No examples in the literature have yet been found on the use of a photoreactor working under high O_2 pressure, which would substantially increase the reaction rate.

5.7. Stoichiometric Threshold. The stoichiometric threshold is defined as the number of moles converted above which a photo-assisted reaction can be considered truly catalytic. The first observation was of the photocatalytic dehydrogenation of aliphatic C_1-C_4 alcohols performed on titania-deposited noble metals [33]. In that reaction, it was demonstrated that titania was the photoactive agent but required a noble metal additive in order to *i*) attract photogenerated electrons, *ii*) neutralize protons to H-atoms, *iii*) recombine the H-atoms to H_2 , and *iv*) desorb H_2 in the gas phase.

Without Pt, titania was able to produce a certain amount of H_2 , but, after a period of *ca.* 1 h depending on the conditions, the evolution of H_2 stopped. The number of moles evolved was considered the stoichiometric threshold, corresponding to the exhaustion of nonrenewable active sites. In presence of Pt, the evolution of H_2 could be performed over long UV-irradiation periods, enabling us to reach conversions $1000 \times$ greater than the photocatalytic threshold without any loss of activity, warranting the catalytic nature of the reactions. Similarly, the liquid-phase oxidation of 4-*tert*-butyltoluene in 4-*tert*-butylbenzaldehyde [17] and cyclohexane in cyclohexanone [16a] gave conversions that exceeded the photocatalytic threshold by factors of 1000 and 100, respectively.

In aqueous media to be detoxified, pollutant concentrations are generally rather low. Since OH^\cdot radicals, originating from the neutralization of OH^- surface groups by photoholes, are generally considered the degrading oxidative species, the stoichiometric threshold has to be determined by calculating the initial number n_0 of OH_s groups:

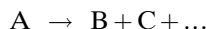
$$n_0 = m \cdot S_{BET} \cdot d$$

where m is the mass of catalyst used, S_{BET} is its surface area and d is the surface OH group density at saturation, which can be taken to be $5 \times 10^{18}/m^2$ according to *Böhm* [13]. For instance, in the solar pilot plant at *PSA*, with 50 g of *Degussa P-25* at $50 m^2/g$, one obtains a maximum initial number of 2.075×10^{-2} mol of OH groups. The total degradation of 1.4×10^{-4} mol/l of herbicide 2,4-D in 250 l corresponded to 3.5×10^{-2} mol [41]. The stoichiometric threshold has been exceeded by a factor of 1.7 for one experiment in dilute medium. Similarly, the photocatalytic degradation of

4-chlorophenol by the titania-activated carbon system reused several times in the same pilot reactor has converted a number of moles 5-fold higher than the stoichiometric threshold without any loss of activity [41].

When it exceeds unity, this parameter ensures that the reaction is truly catalytic. It should be systematically determined, especially when using modified titania, to check whether any additives or modifications really contribute to the catalytic process of the reaction or artificially to parallel side stoichiometric processes.

6. Photocatalytic Quantum Yield. – The concept of photocatalytic quantum yield (POY, ρ) must be clearly defined from the two parent disciplines, photochemistry and catalysis. In photochemistry, the quantum yield is defined as the number of molecules transformed per adsorbed photon [1]. In a given heterogeneous catalytic reaction,



the yield ρ_B in reaction product B is defined as the ratio of the partial conversion τ_B of reactant A to product B to the overall conversion τ of reactant A [44].

$$\rho_B = \tau_B / \tau = [n_B / n_{A_0}] / [(n_{A_0} - n_A) / n_{A_0}] = n_B / n_{A_0} - n_A$$

Presently, for ρ , we have chosen the dynamic definition given by *Braun et al.* [1], with ρ defined as the ratio of the photocatalytic reaction rate to the incident efficient photon flux φ_e :

$$\rho = r / \varphi_e = (-dn/dt) / \varphi_e$$

with r in molecules/s and φ in photons/s or with r in mol/s and φ in *Einstein/s* (1 *Einstein* = 1 mol of photons). Since a photocatalytic system is particularly heterogeneous, including *i*) gas and liquid fluid phases, *ii*) a solid catalyst, and *iii*) the ‘electromagnetic phase’, *i.e.*, the photon flux, the efficient photon flux has to be clearly determined.

Since the reaction rate parallels the absorption spectrum of the photocatalyst, indicating the transition of some electrons from the valence band into the conduction band of the semiconductor catalyst, only efficient photons have to be considered, *i.e.*, those whose energy $h\nu$ is $\geq E_G$ ($E_G = 3.2$ eV for titania, *i.e.*, $\lambda \leq 380$ nm).

The determination of efficient photon flux is based on various chromatic parameters: *i*) the spectral energetic distribution of the UV-lamp in the various light bands, *ii*) the transmittance of the optical window of the photoreactor, or that of an additional filter when a special wavelength range has to be selected to avoid a concurrent photochemical reaction, and *iii*) the absorbance of titania.

The calculations have been made for the UV lamp (*Philips Model HPK 125*) described in [1]. For each UV-ray of the medium-pressure mercury lamp, the relative light power has been recorded from the data provided by *Philips* and multiplied by the transmittance of the UV-filter. This new monochromatic relative light power produced by transmittance through the filter is then normalized for a total polychromatic power light of 1 W. Then, for each ray of the lamp, a monochromatic photon flux φ_i is calculated by dividing the monochromatic normalized light power P_i by the

corresponding quantum energy $h\nu_i$. The sum of these monochromatic fluxes gives the overall photon flux (in photons/s) for an overall light power of 1 W. Subsequently, the total light power received by the photocatalyst the radiant flux Φ has to be measured, with a radiometer. Since the response of the radiometer depends on the wavelength range used, we have calibrated the radiometer against a microcalorimeter. The total power entering the photoreactor P_T is given by: $P_T = \Phi \times S$ where S is the section area of the photoreactor window.

Such a photon flux should not be used to determine P . Only the efficient photon flux should be taken into account and determined for each catalyst. Therefore, each monochromatic photon flux is multiplied by the absorbance (in %) of the catalyst. The sum of all these monochromatic fluxes gives the total efficient photon flux φ_e for a given catalyst. For instance, when using a *Philips HPK 125* UV-lamp and a *Pyrex* optical window that transmits wavelengths $\lambda \leq 290$ nm, one gets an efficient photon flux per watt φ_w for titania of 8.36×10^{17} efficient photons/s/W, and ρ is:

$$\rho = r/\varphi_e = \frac{(-dn_A/dt)}{\varphi_w \Phi S}$$

Since one absorbed photon creates one electron-hole pair that can generate redox processes when they totally dissociate and do not recombine, and, since no radical chain reactions are involved, ρ will be necessarily smaller than unity.

Optimal Conditions for a Maximum PQY. For a given illumination system, the efficient photon flux φ_e being constant, ρ can be only improved by considering the reaction rate r , which varies as a function of the five main parameters described in Fig. 2, *i.e.*, the mass of catalyst, the wavelength, the partial pressure (in gas-phase reactions) or the concentration (in liquid-phase reactions), the temperature (only in 'extreme' conditions for photocatalysis, *i.e.*, either $T < 0^\circ$ or $T > 80^\circ$), and the radiant flux (in W/m²). Therefore, to obtain maximum PQY, one is required to use: *i*) a mass of catalyst at least equal to the optimum mass m_{opt} at the beginning of the plateau of curve $r = f(m)$ (Fig. 2, *a*); *ii*) in a gas-phase reaction, a partial pressure corresponding to a full coverage of the surface to give the maximum reaction rate in a *Langmuir-Hinshelwood* mechanism, or, similarly in a liquid-phase reaction, a concentration high enough to provide full surface coverage; *iii*) a temperature close to the optimum of the *Arrhenius* plot and far from 'extreme' values, *i.e.* below -10° where the reaction becomes limited by the product desorption or above 85° where the reaction becomes limited by the adsorption of the reactant; and *iv*) a radiant flux lower than the value at which r becomes proportional to $\Phi^{1/2}$, indicating that the electron-hole recombination rate prevails over the reaction rate. In the case of the mild oxidation of cyclohexane into cyclohexanone, the limit was found equal to 25 mW/cm² in the photoreactor in Fig. 3.

The kinetic nature of PQY, defined as the ratio of the reaction rate to the efficient photon flux [1] enables one to check whether a reaction is truly catalytic or not. In Fig. 4, which shows H₂ production from alcohols with titania and titania-deposited Pt photocatalysts, the PQY of naked titania is zero after a period of one h, corresponding to exhaustion of the stoichiometric threshold defined above. A mean quantum yield, which would have been based on the number of molecules converted to the number of

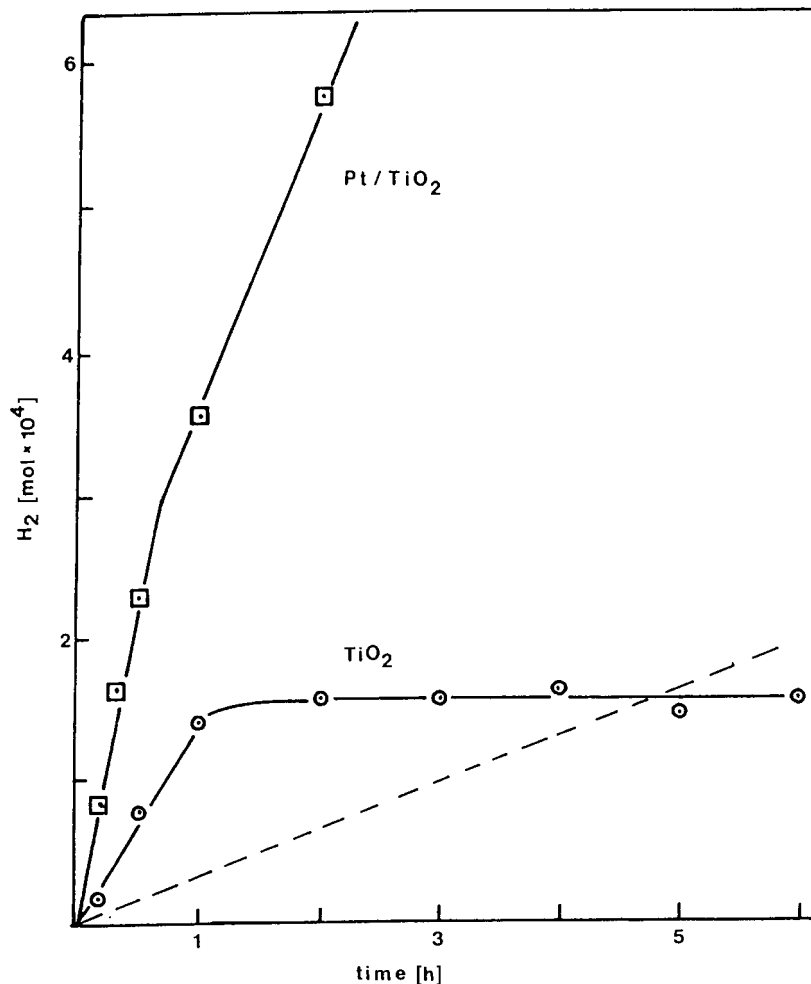


Fig. 4. Hydrogen production from aq. MeOH solution (50:50) with naked titania and by Pt/TiO₂. The dashed line represents the mean rate for naked titania under ca. 5 h of UV-irradiation.

incident photons, would appear permanently positive as indicated by the dashed line in Fig. 4, although the solid is no more active at $t_{UV} > 1$ h.

The Usefulness of PQY. The knowledge of PQY of a given photocatalytic system is particularly interesting for various purposes, enabling one to *i*) compare the catalytic activities of various catalysts in a given reaction under identical conditions, *ii*) establish the relative feasibility of various reactions when performed on the same photocatalyst, and *iii*) calculate the energetic yield involved in a given reaction and the corresponding cost when using artificial light provided by electrical lamps.

7. Conclusions. – Photocatalytic reactions cover a large domain in both organic and inorganic chemistry. Although the basic activation is identical for all systems

considered, very different results can be obtained concerning the selectivity of the reaction. The origin of the differences must be related to the different natures of photoinduced active species, and it has been clearly shown that the crucial parameter is the presence or absence of H₂O. In absence of H₂O, *i.e.*, of regenerable OH surface groups, the generation of dissociated oxygen species prevails and is responsible for mild and selective oxidation processes, especially with hydrocarbons. By contrast, the presence of H₂O saturates the surface of titania with OH⁻ groups, which can be neutralized by positive photoholes into OH[•] radicals, which are known to be strongly oxidative and cracking agents. To each process corresponds a photocatalytic quantum yield, which has been explicitly defined according to the various reaction conditions. This parameter appears to be fundamental to establish whether a photoassisted reaction is really of a photocatalytic nature and to determine the *facile* or *demanding* character of such a reaction.

REFERENCES

- [1] A. M. Braun, M. T. Maurette, E. Oliveros, 'Technologie Photochimique', presses Polytechniques Romandes, Lausanne, 1986.
- [2] 'Photocatalysis and Environment', Ed. M. Schiavello, Kluwer Academic Publisher, Dordrecht, 1988.
- [3] 'Photocatalysis, Fundamentals and Applications', Ed. N. Serpone, E. Pelizzetti, Wiley, New York, 1989.
- [4] 'Photocatalytic Purification and Treatment of Water and Air', Ed. D. F. Ollis, H. Al-Ekabi, Elsevier, Amsterdam, 1993.
- [5] O. Legrini, E. Oliveros, A. M. Braun, *Chem. Rev.* **1993**, *93*, 671.
- [6] J.-M. Herrmann, *Catal. Today* **1999**, *53*, 115.
- [7] D. W. Bahnemann, J. Cunningham, M. A. Fox, E. Pelizzetti, P. Pichat, N. Serpone, in 'Aquatic Surface Photochemistry', Ed. R. G. Zepp, G. R. Helz, D. G. Crosby, F. L. Lewis Publishers, Boca Raton, 1994, p. 261.
- [8] D. M. Blake, 'Bibliography of Work on Photocatalytic Removal of Hazardous Compounds from Water and Air', NREL/TP-430-22197, National Renewable Energy Laboratory, Golden, 1997 and 1999.
- [9] J.-M. Herrmann, J. Disdier, P. Pichat, *J. Chem. Soc., Faraday Trans. 1* **1981**, *77*, 2815.
- [10] P. Pichat, J.-M. Herrmann, H. Courbon, J. Disdier, M. N. Mozzanega, *Can. J. Chem. Eng.* **1982**, *60*, 27.
- [11] a) S. Malato, Ph. D. Thesis, Almeria University, Spain, 1997; b) S. Malato, in 'Solar Photocatalytic Degradation of Pentachlorophenol Dissolved in Water', Coleccion Documentos Ciemat, Madrid, 1999.
- [12] J.-M. Herrmann, *Catal. Today* **1995**, *24*, 157.
- [13] H. P. Böhm, *Adv. Catal.* **1976**, *16*, 179.
- [14] J.-M. Herrmann, H. Courbon, J. Disdier, M. N. Mozzanega, P. Pichat, *Stud. Surf. Sci. Catal.* **1990**, *59*, 675.
- [15] H. Mozzanega, J.-M. Herrmann, P. Pichat, *J. Phys. Chem.* **1979**, *83*, 2251.
- [16] a) W. Mu, J.-M. Herrmann, P. Pichat, *Catal. Lett.* **1989**, *3*, 73; b) J.-M. Herrmann, W. Mu, P. Pichat, *Stud. Surf. Sci. Catal.* **1990**, *55*, 405.
- [17] P. Pichat, J. Disdier, J.-M. Herrmann, P. Vaudano, *Nouv. J. Chim.* **1986**, *10*, 545.
- [18] J.-M. Herrmann, J. Disdier, M. N. Mozzanega, P. Pichat, *J. Catal.* **1979**, *60*, 369.
- [19] H. Courbon, J.-M. Herrmann, unpublished results.
- [20] A. Zafra, J. Garcia, A. Milis, X. Domenech, *J. Mol. Catal.* **1991**, *70*, 343.
- [21] Y. Hori, A. Nakatsu, S. Susuki, *Chem. Lett.* **1985**, 1429.
- [22] J.-M. Herrmann, unpublished results.
- [23] S. N. Frank, A. J. Bard, *J. Phys. Chem.* **1977**, *81*, 1484.
- [24] J.-M. Herrmann, J. Disdier, P. Pichat, *J. Catal.* **1988**, *113*, 72.
- [25] S. N. Frank, A. J. Bard, *J. Am. Chem. Soc.* **1977**, *99*, 303.
- [26] H. Hidaka, T. Nakamura, A. Ishizaha, M. Tsuchiya, J. Zhao, *J. Photochem. Photobiol., A* **1992**, *66*, 367.
- [27] C. H. Pollema, J. L. Hendrix, E. B. Milosavljevic, L. Solujic, J. H. Nelson, *J. Photochem. Photobiol., A* **1992**, *66*, 235.
- [28] J.-M. Herrmann, J. Disdier, P. Pichat, *J. Phys. Chem.* **1986**, *90*, 6028.

- [29] E. Borgarello, N. Serpone, G. Eno, R. Harris, E. Pelizzetti, C. Minero, *Inorg. Chem.* **1986**, 25, 4499.
- [30] E. Borgarello, R. Harris, N. Serpone, *Nouv. J. Chim.* **1985**, 9, 743.
- [31] N. Serpone, E. Borgarello, M. Barbeni, E. Pelizzetti, P. Pichat, J.-M. Herrmann, M. A. Fox, *J. Photochem.* **1987**, 36, 373.
- [32] H. Courbon, J.-M. Herrmann, P. Pichat, *J. Catal.* **1985**, 95, 539.
- [33] P. Pichat, J.-M. Herrmann, J. Disdier, H. Courbon, M. N. Mozzanega, *Nouv. J. Chim.* **1981**, 5, 27; P. Pichat, J.-M. Herrmann, J. Disdier, H. Courbon, M. N. Mozzanega, *Nouv. J. Chem.* **1982**, 6, 53.
- [34] J. Casado, J.-M. Herrmann, P. Pichat, in 'Transport and Transformation of Pollutants in the Troposphere', Ed. P. Borrell, P. M. Borrell, W. Seiler, SPB Academic Publishing, The Hague, 1991, p. 307.
- [35] F. Juillet, F. Lecomte, H. Mozzanega, S. J. Teichner, A. Thévenet, P. Vergnon, *Faraday Discuss., Symp. Chem. Soc.* **1973**, 7, 57.
- [36] S. Malato Rodríguez, J. Blanco Gálvez, J.-M. Herrmann, *Catal. Today* **1999**, 54, 191 (Introduction by the Guest Editors to the Special Issue on Solar Photocatalysis).
- [37] C. S. Turchi, D. F. Ollis, *J. Catal.* **1989**, 119, 483.
- [38] J.-M. Herrmann, M. Gravelle-Rumeau-Mailleau, P. C. Gravelle, *J. Catal.* **1987**, 104, 136.
- [39] C. S. Turchi, M. Mehos, J. Pacheco, in 'Photocatalytic Purification and Treatment of Water and Air', Ed. D. F. Ollis, H. Al-Ekabi, Elsevier, Amsterdam, 1993.
- [40] R. Miller, R. Fox, in 'Photocatalytic Purification and Treatment of Water and Air', Ed. D. F. Ollis, H. Al-Ekabi, Elsevier, Amsterdam, 1993, p. 573.
- [41] J.-M. Herrmann, J. Matos, J. Disdier, C. Guillard, J. Laine, S. Malato, J. Blanco, *Catal. Today* **1999**, 54, 255.
- [42] J. E. Germain, in 'La Catalyse de Contact', les Techniques de l'Ingénieur, Série J 1181, 1979, p. 11.

Received June 2, 2001